

Self similarity of the dark matter dominated objects and the shape of small scale power spectrum

M. Demiański^{a,b,*}, A. Doroshkevich^{c,d†}

^aInstitute of Theoretical Physics, University of Warsaw, 02-003, Warsaw Poland

^bDepartment of Astronomy, Williams College, Williamstown, MA 01267, USA

^cLebedev Physical Institute of Russian Academy of Sciences, 117997, Moscow, Russia

^dNational Research Center Kurchatov Institute, 123182, Moscow, Russia

October 13, 2018

Abstract

We analyzed available observational data of a sample of dark matter (DM) dominated galaxies and clusters of galaxies and we have found correlations between the virial mass, M_{vir} , of halos and basic parameters of their cores, namely, the mean DM density, pressure and entropy. These correlations are a natural consequence of similar evolution of all such objects. It is driven mainly by gravitational interactions what implies a high degree of self similarity of both the process of halos formation and their internal structure.

We confirmed the CDM-like shape of both the small and large scale power spectrum. However, our reconstruction of the evolutionary history of observed objects requires either a multicomponent composition of DM or a more complex primordial power spectrum of density perturbations with significant excess of power at scales of clusters of galaxies and larger. We demonstrated that a model with suitable combination of the heavy DM particles (CDM) and DM particles with large damping scale (HDM) could provide a successful description of the observational data in a wide range of masses.

Keywords: Cosmology: formation of DM halos, galaxies and clusters of galaxies – initial power spectrum – composition of dark matter

1 Introduction

One of the important goals of cosmology is to establish correlations between the observed Universe – the CMB, Large Scale Structure (LSS), galaxies etc. – and the processes that occurred at the earlier epochs of evolution of the Universe and are encoded in the initial power spectrum of density perturbations. For larger scale $D > 10Mpc$ this problem is approximately solved by the CMB observations of the WMAP (Komatsu et al. 2011; Hinshaw et al. 2013) and Planck (Ade et al. 2016) missions and is realized as the standard Λ CDM model. However the shape of the power spectrum at small scale remains unknown and its investigation is one of the actual current problem of cosmology. Now it is unfortunately not possible to obtain reliable information about this very important issue. Next very interesting problem is the universality and the self similarity of the internal structure of DM dominated halos in a wide range of their masses and sizes.

To discuss these problems we use the improved quantitative descriptions of observed characteristics of DM dominated objects – dSph and Ultra Diffuse (UDG) galaxies, and clusters of galaxies – for which we can expect the relatively weak contribution of baryonic component. As usual we will characterize such virialized objects by their virial mass, M_{vir} , which is the most popular basic characteristic of objects in spite of the low precision of its observational determination. We also use the well known correlation between the virial masses of DM dominated objects and the period (or redshift) of their formation. The DM dominated objects attract our attention as their evolution is driven by gravitational forces only and thus it is the simplest one as compared with the complex evolution of numerous baryon dominated galaxies.

*Marek.Demianski@fuw.edu.pl

†dorr@asc.rssi.ru

The relict concentration of baryons is moderate ($\sim 16\%$) and its influence on the object evolution is also weak. However this influence is strongly enhanced for the most abundant objects with virial masses $\sim 10^9 \leq M_{vir}/M_\odot \leq 10^{13}$ and virial velocities $\sim 15\text{km/s} \leq v_{vir} \leq 400\text{km/s}$. For such objects the heating of baryons by shock waves, subsequent cooling and infall into central region strongly distort their internal structure and lead to formation of Irr, spiral and elliptical galaxies. These processes are not so efficient for dwarf galaxies with the low virial temperature $T_{vir} \leq 1.5 \cdot 10^4\text{K}$ and clusters of galaxies with the high virial temperature $T_{vir} \geq 10^7\text{K}$ and low density of baryons.

Evidently the halo formation is a deterministic process and properties of virialized objects correlate with properties of the initial perturbations. However, the complex character of the process of halo formation (see, e.g. Demiański et al. 2011) destroys many correlations. Simulations show that for the DM dominated objects which evolve mostly due to gravitational interactions the more stable characteristics are the object rotation and the internal structure of their central regions – the mean density, pressure and entropy of their cores. It can be expected that these characteristics are moderately distorted in the course of halos formation and evolution and they can be linked with properties of initial perturbations.

Properties of both simulated and observed DM dominated virialized objects are usually described in the framework of spherical models such as the Navarro – Frenk – White (NFW) proposal Navarro et al. (1997), isothermal or Burkert (1995) models. This approach allows to discuss and to link together both the general parameters of a halo, such as its virial mass, period of its formation, relations between the thermal and gravitational energy, and its internal properties. This approach allows to obtain a very simple, though rough, general description of the process of DM halos formation and introduces some hierarchy of formed objects. To illustrate problems of this approach we can refer to the papers of Weisz et al. (2014) where reconstructions of evolution are presented for several dwarf galaxies. High differences of these evolutionary tracks emphasize the problems arising for our analysis and explain the unavoidable scatter of resulting estimates.

This analysis also reveals a possible deviations of the main observed characteristics from expectations based on standard assumptions about the DM composition and/or initial power spectrum used in theoretical models and simulations. An example of such deviation is the 'To Big to Fail' effect (Boylan–Kolchin et al. 2012; Garrison–Kimmel et al., 2014a,b; Tollerud et al. 2014; Klypin et al. 2015; Hellwing et al. 2015; Brook, & Cintio 2015), what indicates that the usually accepted models should be improved.

Of course, our approach is the first and very rough quantitative approximation. More extended discussion of these problems can be found in Demiański & Doroshkevich (2015). Evidently these results will be discussed and corrected many times as new observations and special simulations will become available.

1.1 Cosmological parameters

In this paper we consider the spatially flat Λ dominated model of the Universe with the Hubble parameter, $H(z)$, the mean critical density $\langle \rho_{cr} \rangle$, the mean density of non relativistic matter (dark matter and baryons), $\langle \rho_m(z) \rangle$, and the mean density and mean number density of baryons, $\langle \rho_b(z) \rangle$ & $\langle n_b(z) \rangle$, given by Komatsu et al. 2011, Hinshaw et al. 2013:

$$H^2(z) = H_0^2[\Omega_m(1+z)^3 + \Omega_\Lambda], \quad H_0 = 100h \text{ km/s/Mpc},$$

$$\langle \rho_b(z) \rangle = \frac{3H_0^2}{8\pi G}\Omega_b(1+z)^3 \approx 4 \cdot 10^{-31}(1+z)^3 \Theta_b \frac{g}{\text{cm}^3}, \quad \Theta_b = \frac{\Omega_b h^2}{0.02}, \quad (1)$$

$$\langle \rho_m(z) \rangle = 2.5 \cdot 10^{-30}(1+z)^3 \Theta_m \frac{g}{\text{cm}^3} = 34(1+z)^3 \Theta_m \frac{M_\odot}{\text{kpc}^3}, \quad \Theta_m = \frac{\Omega_m h^2}{0.12},$$

Here $\Omega_m = 0.24$ & $\Omega_\Lambda = 0.76$ are the mean dimensionless density of non relativistic matter and dark energy, $\Omega_b \approx 0.04$ and $h = 0.7$ are the dimensionless mean density of baryons, and the dimensionless Hubble constant measured at the present epoch. Cosmological parameters presented in the recent paper of the Planck collaboration (Ade et al. 2016) slightly differ from those used above.

For this model with $\Omega_m \approx 0.25$ the evolution of perturbations can be described with sufficient precision by the expression

$$\delta\rho/\rho \propto B(z), \quad B^{-1}(z) \approx \frac{1+z}{1.35} [1 + 1.44/(1+z)^3]^{1/3}. \quad (2)$$

(Demiański & Doroshkevich, 1999, 2004, 2014; Demiański et al. 2011). For $z = 0$ we have $B = 1$ and for $z \geq 1$, $B(z)$ is reproducing the exact function with accuracy better than 90%. For $z \geq 1$ these relations

simplify. Thus, for the Hubble constant and the function $B(z)$ we get

$$H^{-1}(z) \approx \frac{0.85 \cdot 10^{18} \text{s}}{\sqrt{\Theta_m}(1+z)^{3/2}}, \quad B(z) \approx \frac{1.35}{1+z}. \quad (3)$$

2 Physical model of halos formation

2.1 DM density in virialized halos

In this paper we assume that all relaxed DM halos are described by the NFW density profile

$$\rho(x) = \frac{\rho_0}{x(1+x)^2}, \quad x = r/r_s, \quad (4)$$

where $\rho_0(M_{vir})$, & $r_s(M_{vir})$ are model parameters. Using this density we get that

$$\begin{aligned} M(r) &= M_s f_m(r/r_s), \quad M_s = 4\pi\rho_0 r_s^3, \quad M_{vir} = M_s f_m(c), \\ f_m(x) &= \ln(1+x) - x/(1+x), \quad c = R_{vir}/r_s \geq 3, \\ M(r_s) &= M_s f_m(1) \approx 0.2M_s, \end{aligned} \quad (5)$$

where c is the concentration and R_{vir} is the halo virial radius. For the mean density of halos, $\langle\rho_{vir}\rangle$ and the mean density of their central core $\langle\rho_s\rangle$ we get

$$\begin{aligned} \langle\rho_{vir}\rangle &= 3M(R_{vir})/4\pi R_{vir}^3 = 3\rho_0 f_m(c)/c^3, \\ \langle\rho_s\rangle &= 3M(r_s)f_m(1)/4\pi r_s^3 \approx 0.6\rho_0, \end{aligned}$$

and finally we have

$$\langle\rho_s\rangle = 5.4\langle\rho_{vir}\rangle \left(\frac{c}{3}\right)^3 \frac{1}{f_m(c)}. \quad (6)$$

These relations link together the fundamental characteristics of halos, namely, their mean density, concentration and masses. Moreover as the function $f_m(c)$ is a slowly varying function of c than for the most interesting population of objects we can neglect the differences between M_{vir} and M_s :

$$4 \leq c \leq 8, \quad 0.8 \leq f_m(c) \leq 1.3,$$

$$M_{vir} \approx M_s(1 \pm 0.25) \approx 5M(r_s)(1 \pm 0.25). \quad (7)$$

These relations allow to roughly estimate the parameters of observed objects in spite of scarcity of observational data.

2.2 The redshift of halo formation

For each mass of DM halo its formation is a complex process extended in time, what causes some ambiguity in the halo parameters such as its virial mass and the epoch or redshift of its formation (see, e.g. discussion in Partridge & Peebles 1967a,b; Peebles 1980; and more recently Kravtsov & Borgani 2012). The main stages of this process can be investigated in details with numerical simulations (see, e.g. Demiański et al. 2011). The analytic description of this process is however problematic.

For a virialized DM halo of mass M_{vir} the redshift (or epoch) of its formation, z_f , and the corresponding mean DM density $\langle\rho_{vir}\rangle$ were roughly estimated by Partridge & Peebles (1967a,b) and were later determined more accurately in the framework of the simple *phenomenological* toy models (Zel'dovich & Novikov 1983; Lacey & Cole 1993; Bryan & Norman 1998). According to these models the virial density is proportional to the mean density (1) at the moment of object formation,

$$\begin{aligned} \langle\rho_{vir}\rangle &= 18\pi^2\langle\rho_m(z_f)\rangle \approx \rho_{200}(1+z_f)^3, \\ \rho_{200} &= 200\langle\rho_m(0)\rangle = 0.68 \cdot 10^4 M_\odot/kpc^3 = 5 \cdot 10^{-28} g/cm^3. \end{aligned} \quad (8)$$

In the Lacey – Cole model halos are considered as formed at the moment of collapse of homogeneous spherical DM clouds and they are described by the adiabatic Emden model with $\gamma = 5/3$, $n = 3/2$ (Peebles 1980; Zel'dovich & Novikov 1983).

The advantage of this approach is its apparent universality and reasonable results that are obtained for massive clusters of galaxies. However, both its precision and range of applicability are limited owing to noted simplified assumptions. Thus, even the numerical coefficient $18\pi^2$ is determined by the Emden model for halo description. An important, but usually ignored, special feature of the Lacey - Cole model is the strong mass dependence of the virial density,

$$\langle \rho_{vir} \rangle \propto M_{vir}^{-2}, \quad (1 + z_f) \propto M_{vir}^{-2/3}. \quad (9)$$

Attempts to use these relations for unified description of observed DM halos of galactic and clusters scales immediately leads to unacceptable results. Thus, expectations of the model (8,9) are in contrast with the weaker mass dependence of the observed parameters of DM dominated objects (sections 4). It is also important that for dSph galaxies Eq. (8) leads to a very high value of $z_f \sim 15$, what exceeds both the age of dSph galaxies derived from observations of stars (see, e.g., Weisz et al. 2014; Karachentsev et al., 2015) and the redshift of reionization $z_{reio} \sim 9$ determined by Planck (Ade 2016). Nonetheless the main significance of the Lacey – Cole model (8) is the clear introduction of the concept of the epoch (or redshift z_f) of halo formation, what allows us to quantify correlation of halo parameters with the process of growth of perturbations and halo formation.

Evidently the basic assumptions of the simple model (8) are not realistic. Indeed the processes of merging and anisotropic matter accretion unpredictably changes the density. Analysis of high resolution simulations (Demiański et al. 2011) shows that influence of these random factors together with the strong anisotropy of the early period of DM halo formation depends upon the halo mass and, for example, it is moderate for clusters of galaxies. It is accepted that for the simple Λ CDM cosmological model and for more massive objects the expression (8) describes reasonably well both the observations and simulations. However, the formation of low mass objects is regulated by other factors and thus their structure cannot be described by the same relations. These comments attempt to explain the main reasons why the model (8,9) has limited applicability.

In order to describe the complex process of DM halo formation in a wide range of virial masses of objects we use the more general *phenomenological* relation

$$\langle \rho_{vir} \rangle = 18\pi^2 \Phi(M_{vir}) \langle \rho_m(z_f) \rangle \approx \rho_{200} \Phi(M_{vir}) (1 + z_f)^3, \quad (10)$$

where $\Phi(M_{vir}) \geq 1$ is a smooth slowly varying function of M_{vir} . This relation preserves the universality of (8) and provides an unified self consistent description of observed properties of DM halos in a wide range of masses $10^6 \leq M_{vir}/M_\odot \leq 10^{15}$. In particular, it reproduces the observed weak mass dependence of the redshift z_f and the density $\langle \rho_{vir} \rangle$ for both clusters of galaxies and low mass THINGS, LSB, UDG and dSph galaxies. Further discussion of these problems can be found below in sections 3, and 4.

Precise observations of DM periphery of both clusters and galaxies are problematic owing to the strongly irregular matter distribution in their outer regions. Hence, we use only estimates of the more stable parameter - the virial mass of object as its leading characteristic. For example, sometimes the relation (8) is used for description of clusters of galaxies under the arbitrary assumption that the cluster is formed at the observed redshift, $1 + z_f \equiv 1 + z_{obs}$. In this case the relation (8) allows to determine formally the mean virial density $\langle \rho_{vir} \rangle$ and, for a given mass of cluster M_{vir} , its virial radius, R_{vir} . However, this result is evidently incorrect because, in fact, we can only conclude that $z_f \geq z_{obs}$, what is trivial for galaxies. For clusters the difference between $1 + z_f$ and $1 + z_{obs}$ can be as large as $\sim 1.5 - 2$.

More stable and refined method to determine the redshift of halo formation uses characteristics of the halo core rather than its periphery. In this case we use the following expression for the concentration

$$c(M_{vir}, z_f) \approx 0.12 M_{12}^{1/6} (1 + z_f)^{7/3}, \quad M_{12} = \frac{M_{vir}}{10^{12} M_\odot}, \quad (11)$$

(Demiański & Doroshkevich 2014). Together with relations (6) and (10) we get for the mean density of the central core

$$\langle \rho_s \rangle = \rho_{cc} M_{12}^{1/2} (1 + z_f)^{10} \Phi(M_{vir}), \quad (12)$$

$$\rho_{cc} = 0.38 \cdot 10^{-3} \frac{\rho_{200}}{f_m(c)} \approx \frac{2.5}{f_m(c)} \frac{M_\odot}{kpc^3} = \frac{1.9}{f_m(c)} \cdot 10^{-31} \frac{g}{cm^3}.$$

This relation links the redshift z_f with the virial mass M_{vir} and the mean density of halo core $\langle \rho_s \rangle$ and allows to determine z_f . Application of this approach requires additional observations. However, it is less

sensitive to random deviations of characteristics of periphery of objects. Moreover for DM dominated high density objects observed at $z_{obs} \ll 1$ (such as the dSph galaxies) determination of the redshift z_f through the parameters of the central core is also preferred.

The main weakness of this approach is the possible impact of baryonic component that can be specially important for galaxies with moderate DM domination. However, for dSph galaxies this effect can be comparable with the uncertainties in measurements of parameters, what is clearly seen, when one compares the results presented in Walker et al. (2009) and Kirby et al. (2014) (see section 4).

Comparison of (10) and (12) indicates that the density of halo core $\langle \rho_s \rangle$ is more sensitive than $\langle \rho_{vir} \rangle$ to both the virial mass and the redshift of formation. However, for all observed samples (section 4) z_f is correlated with M_{vir} :

$$\eta_f = (1 + z_f)M_{12}^{0.077} \approx 4.1(1 \pm 0.1), \quad (13)$$

(see also Demiański & Doroshkevich 2014). Allowing for this correlation we see from (12) that actually $\langle \rho_s \rangle$ is a weak function of both the virial mass M_{vir} and the redshift of formation z_f .

2.3 Excursion set approach and shape of the power spectrum

It is well known that at redshifts $z \geq 3$ the formation of galactic scale halos dominates, but the typical mass of halos increases with time and massive clusters of galaxies are formed later at redshifts $z \leq 2$. This correlation between the redshift of halo formation z_f and the halo mass M_{vir} is described by current models of halo formation (Press & Schechter 1974; Bardeen et al. 1986; Bond et al. 1991; Sheth & Tormen 2002; 2004). They are based on the excursion set approach applied to the initially Gaussian random density perturbations. They reduce description of characteristics of the formed halos to the problem of crossing of an appropriate barrier by particles undergoing Brownian motion. A close link between the power spectrum and properties of DM halos and Large Scale Structure had been demonstrated in many simulations.

All theoretical models of halos formation predict that the distribution functions of halo characteristics are dominated by a typical Gaussian term:

$$dP(M_{vir}) \propto \exp[-\alpha \Psi^2(M_{vir})] dM_{vir}, \quad (14)$$

$$\Psi(M_{vir}) = \sigma_m(M_{vir})B(z_f(M_{vir})),$$

where $B(z_f)$ (3) describes the growth of density perturbations and σ_m is the dispersion of density perturbations given by

$$\sigma_m^2(M) = \frac{1}{2\pi} \int_0^\infty k^2 p(k) W^2(k, M) dk, \quad (15)$$

$$W(x) = 3(\sin x/x^3 - \cos x/x^2), \quad x = kr \propto kM^{1/3}.$$

Here $p(k)$ is the power spectrum and W is the Fourier transform of the real-space top-hat filter corresponding to a spherical mass M . Thus, the function $\Psi(M_{vir})$ characterizes the amplitude of perturbations with mass M_{vir} . The usually used condition

$$\Psi(M_{vir}) = \sigma_m(M_{vir})B(z_f(M_{vir})) \approx const, \quad (16)$$

provides the expected approximate self similarity of the process of halo formation and progressive growth with time of the virial mass of halos.

For the CDM – like power spectrum and for the standard normalization of perturbations on σ_8 the function σ_m and α are well fitted by the following expressions

$$\sigma_m = \frac{3.31\sigma_8 M_{12}^{-0.077}}{1 + 0.177M_{12}^{0.133} + 0.16M_{12}^{0.333}}, \quad \alpha = \frac{1.686^2}{2\sqrt{2}} \approx 1, \quad (17)$$

where $M_{vir} = M_{12}10^{12}M_\odot$, 1.686 is the critical overdensity (height of the barrier) and $\sigma_m \approx \sigma_8$ for

$$M_{12} = \frac{4\pi}{3} \frac{\langle \rho_m \rangle}{10^{12}M_\odot} \left(\frac{8Mpc}{h} \right)^3 \approx 210\Theta_m \left(\frac{0.7}{h} \right)^3.$$

It is interesting that for $M_{12} \leq 1$ we get from (3), (13), and (17) that

$$\Psi(M_{vir}) \approx \frac{4.47\sigma_8}{(1 + z_f)M_{12}^{0.077}} = 1.1\sigma_8 \left(\frac{4.1}{\eta_f} \right) \approx const, \quad (18)$$

what is consistent with (16) and demonstrates that properties of low mass objects are in agreement with the CDM-like shape of the small scale power spectrum. We will discuss in more details the observed properties of the function $\Psi(M_{vir})$ in section 5.

3 Expected properties of the relaxed DM halos

We consider the DM halos as a one parametric sequence of objects all properties of which depend upon their virial mass. This means that we consider all DM halos as similar ones. Together with the virial characteristics of halos, namely, the mass, M_{vir} , radius R_{vir} , and density $\langle\rho_{vir}\rangle$ we also consider the mean characteristics of their central cores, namely, the density $\langle\rho_s\rangle$, pressure, $\langle P_s\rangle$, temperature $\langle T_s\rangle$ and entropy $\langle S_s\rangle$. The very important characteristic of a halo is the redshift of its formation, z_f , that was introduced by (10), it approximately characterizes the end of the period of halo formation and relaxation.

The DM temperature and velocity dispersion σ_v in the core usually are not observed, but within relaxed DM cores σ_v is close to the circular velocity, $v_c(r)$, (Demiański & Doroshkevich 2014)

$$\sigma_v^2(r) \approx v_c^2(r) \sqrt{r_s/r}. \quad (19)$$

Because of this we can estimate the expected central parameters of a DM halo as:

$$\begin{aligned} \langle T_s \rangle &\approx \frac{m_b v_c^2}{2} \approx 1.8 eV M_{12}^{5/6} (1+z_f)^{10/3} (\Phi/f_m)^{1/3} \mu_{DM}, \\ \langle P_s \rangle &\approx 10^{-7} eV/cm^3 M_{12}^{4/3} (1+z_f)^{40/3} (\Phi/f_m)^{4/3}, \\ \langle S_s \rangle &\approx 80 cm^2 keV \frac{M_{12}^{1/2}}{(1+z_f)^{10/3}} \mu_{DM}^{5/3} (f_m/\Phi)^{1/3}. \end{aligned} \quad (20)$$

Using the correlation between z_f and M_{vir} (13) we finally get

$$\begin{aligned} \langle \rho_s \rangle &\approx \eta_\rho M_{12}^{-0.2} \frac{\Phi}{f_m} \left(\frac{\eta_f}{4.1} \right)^{10}, \\ \langle P_s \rangle &\approx \eta_p M_{12}^{0.4} \left(\frac{\Phi}{f_m} \right)^{4/3} \left(\frac{\eta_f}{4.1} \right)^{40/3}, \\ \langle S_s \rangle &\approx \eta_s M_{12}^{0.73} \left(\frac{\eta_f}{4.1} \right)^{-10/3} \left(\frac{f_m}{\Phi} \right)^{1/3} \mu_{DM}, \end{aligned} \quad (21)$$

where expected values of the constants are

$$\eta_\rho \approx 2.6 \cdot 10^6 \frac{M_\odot}{kpc^3}, \quad \eta_p \approx 22 \frac{eV}{cm^3}, \quad \eta_s \approx 0.9 cm^2 keV. \quad (22)$$

The expected self similar character of the internal structure of DM cores is manifested by a weak dependence of the parameters η_f , η_ρ , η_p , & η_s upon the virial mass of objects in a wide range of masses. For the observed objects values of these parameters are obtained in the next section 4. For the best sample of 19 dSph galaxies with $M_{vir} \leq 10^9 M_\odot$ and 19 CLASH clusters with $M_{vir} \geq 10^{14} M_\odot$ we have

$$\eta_\rho \approx 1.3 \cdot 10^6 (1 \pm 0.9) \frac{M_\odot}{kpc^3}, \quad \eta_s \approx 1.2 (1 \pm 0.5) cm^2 keV, \quad \eta_f \approx 4.1 (1 \pm 0.1), \quad (23)$$

what is quite similar to expectations (22). Here and below we use the correction factor

$$\Phi(M_{vir}) = (1 + M_f/M_{vir})^{0.3}, \quad M_f \approx 8 \cdot 10^{12} M_\odot, \quad (24)$$

that allows us to obtain an unified self consistent description of both discussed galaxies and clusters of galaxies. Thus, for larger masses $M_{vir} \gg M_f$, $\Phi \rightarrow 1$, and expressions (8) and (10) become identical to each other. On the other hand, in the opposite case $M_{vir} \ll M_f$ the function (24) allows to reconcile theoretical expectations (21) with observations (33) presented in section 4. For low mass dSph galaxies this approach decreases the redshift of formation z_f down to values consistent with the observed age of stars and Planck estimates of the redshift of reionization.

Of course the function $\Phi(M_{vir})$ (24) should be considered only as the first approximation. But to obtain more refined and justified description of the redshift of formation z_f (10) and DM halo parameters (21) we need to have both richer observational data with only moderate scatter and corresponding high resolution simulations.

As is seen from (13) and (11) the so defined concentration is only weakly depended on the virial mass,

$$\langle c \rangle \approx 3(\eta_f/4.1)^{7/3} M_{12}^{0.004}. \quad (25)$$

4 Observed characteristics of DM dominated galaxies and clusters of galaxies

For our analysis we used more or less reliable observational data for ~ 19 DM dominated clusters of galaxies, one UDG and ~ 30 dSph galaxies. For comparison we use also observations of 30 groups of galaxies and ~ 11 THINGS and LSB galaxies. In this section we consider properties of the central cores of virialized DM halos using the approximations summarized in the previous sections. We characterize halos by their virial mass M_{vir} and redshift of formation, z_f . We assume that at $z \leq z_f$ the halos mass and core temperature and density do not change significantly.

4.1 The CLASH clusters

For 19 clusters of the CLASH sample (Merten et al. 2015) in addition to the usually presented observed virial mass of clusters, M_{vir} , there are also estimates of the size and density of central core, r_s , & ρ_0 . For this survey the published parameters R_{vir} , & ρ_{vir} are obtained under the assumption that $z_f = z_{obs}$ and they are not used in our analysis. The virial mass of clusters, M_{vir} , presented in Merten et al. (2015) is close to the estimates of M_{vir} obtained by Umetsu et al. (2014), what confirms reliability of these estimates.

For these clusters parameters of cores can be used without serious corrections. Main results are plotted in Figs. 1 and 2. We get for this survey

$$\langle c \rangle \approx 3.7(1 \pm 0.2), \quad \langle 1 + z_f \rangle \approx 2.3(1 \pm 0.1), \quad \langle \eta_f \rangle \approx 3.9(1 \pm 0.1), \quad (26)$$

$$\langle \rho_s \rangle \approx 5 \cdot 10^5 (1 \pm 0.5) M_\odot / kpc^3, \quad \langle \eta_\rho \rangle \approx 1.6 \cdot 10^6 (1 \pm 0.5) M_\odot / kpc^3,$$

$$\langle S_s \rangle \approx 160(1 \pm 0.9) cm^2 keV, \quad \langle \eta_s \rangle \approx 1.2(1 \pm 0.1) cm^2 keV,$$

$$\langle M_{12} \rangle \approx 10^3, \quad \langle \Psi(M) \rangle \approx 0.4\sigma_8(1 \pm 0.1). \quad (27)$$

4.2 Ultra diffuse galaxies

Now there are new possibilities of observations of the Ultra Diffuse Galaxies (UDG) (Liu et al. 2015; Beasley et al. 2016; Martinez-Delgado et al. 2016). For one of this object – DM dominated galaxy Dragonfly 44 (van Dokkum et al. 2016) – there are observations of $M_{1/2}$, $r_{1/2}$, & σ_v what allows us to repeat the analysis performed for the dSph galaxies. Thus, we get for this galaxy

$$c = 2.8 \quad 1 + z_f \approx 5.2, \quad \eta_f \approx 3.8, \quad M_{vir} \approx 1.4 \cdot 10^{10} M_\odot, \quad (28)$$

$$\rho_s \approx 4.2 \cdot 10^8 M_\odot / kpc^3, \quad \eta_\rho \approx 2.4 \cdot 10^7 M_\odot / kpc^3,$$

$$S_s \approx 0.078 cm^2 keV, \quad \eta_s \approx 3.3 cm^2 keV, \quad \Psi(M) \approx 1.1\sigma_8,$$

These data are presented in Figs. 1&2. As is seen from these Figures this galaxy is located halfway between the CLASH clusters and dSph galaxies and quite well fits with other data plotted in these Figures. This can be considered as the independent evidence in favor of our approach and inferences. We hope that further investigations of UDG galaxies will improve our results.

4.3 Two catalogues of the dSph galaxies

Recently the main observed parameters the dSph galaxies were listed and discussed in many papers. Published characteristics of these galaxies vary from paper to paper and are presented with significant scatter. From samples presented in Walker et al. (2009 & 2011); Collins et al. (2014); Tollerud et al. (2012 & 2014) we selected 19 objects with high DM density, what suggests that these objects were formed at high redshifts and can be considered as samples of earlier galaxies responsible for reionization. This means that for these galaxies the redshift of formation z_f should be comparable with redshift of reionization $z_{reio} \sim 9$ determined by WMAP and Planck missions. For these galaxies we find

$$\begin{aligned} \langle c \rangle &\approx 3.7(1 \pm 0.2), & \langle 1 + z_f \rangle &\approx 9.9(1 \pm 0.1), & \langle \eta_f \rangle &\approx 4.2(1 \pm 0.1), \\ \langle \eta_\rho \rangle &\approx 2.2 \cdot 10^5(1 \pm 0.7)M_\odot/kpc^3, & \langle \eta_s \rangle &\approx 0.9(1 \pm 0.3)cm^2keV, \\ 10^6 &\leq M_{vir}/M_\odot \leq 10^8, & \langle \Psi(M) \rangle &\approx 1.1(1 \pm 0.1)\sigma_8. \end{aligned} \quad (29)$$

Other results for this survey are plotted in Figs 1 & 2.

Second catalog of dSph galaxies (Kirby et al. 2014) contains 30 satellites of Milky Way and Andromeda with independent measurements of their parameters. Some of them significantly differ from those presented in Walker et al. (2009 & 2011) and Tollerud et al. (2012 & 2014). We have for this survey

$$\begin{aligned} \langle c \rangle &\approx 3.3(1 \pm 0.2), & \langle 1 + z_f \rangle &\approx 8.1(1 \pm 0.1), & \langle \eta_f \rangle &\approx 4.1(1 \pm 0.1), \\ \langle \eta_\rho \rangle &\approx 1.5 \cdot 10^5(1 \pm 0.7)M_\odot/kpc^3, & \langle \eta_s \rangle &\approx 1.1(1 \pm 0.4)cm^2keV, \\ 10^6 &\leq M_{vir}/M_\odot \leq 10^8, & \langle \Psi(M) \rangle &\approx 1.1(1 \pm 0.1)\sigma_8. \end{aligned} \quad (30)$$

Other results for this survey are plotted in Figs 1 & 2. This comparison of results (29) and (30) allows to verify representativity and reliability of obtained estimates.

4.4 The groups of galaxies

For comparison parameters of 30 suitable groups of galaxies with $z_{obs} \ll 1$ are taken from the catalog of Makarov & Karachentsev (2011). For these objects we cannot identify the central core. But these data allow us to estimate – with large scatter – the mean density and the redshift of formation as

$$\begin{aligned} 1.2 \leq M_{12} \leq 200, & \quad 100kpc \leq R_{vir} \leq 700kpc, & \langle \rho_{vir} \rangle &\approx 2.7 \cdot 10^5(1 \pm 0.9)M_\odot/kpc^3, \\ \langle 1 + z_f \rangle &\approx 3.1(1 \pm 0.3), & \langle \eta_f \rangle &\approx 3.1(1 \pm 0.3), & \langle \Psi(M) \rangle &\approx 0.74\sigma_8(1 \pm 0.3), \end{aligned} \quad (31)$$

and to fill partly the empty region in Fig. 2 between the galaxies and clusters of galaxies. Main results of our analysis are plotted in Fig. 2.

4.5 The THINGS and LSB galaxies

For 11 LSB and THING galaxies (de Blok et al. 2008; Kuzio de Naray et al. 2008) the observed rotation curves are measured up to large distances, what allows us to estimate, with a reasonable reliability, the virial masses M_{vir} and the mean virial density, $\langle \rho_{vir} \rangle$, and, finally, using the relation (10) to estimate the redshift of formation and the virial mass of these objects. we get

$$\begin{aligned} \langle 1 + z_f \rangle &\approx 2.3(1 \pm 0.3), & \langle \eta_f \rangle &\approx 2.8(1 \pm 0.3), & \langle M_{12} \rangle &\approx 0.24(1 \pm 0.8), \\ \langle \rho_{vir} \rangle &\approx 6.2 \cdot 10^5(1 \pm 0.9)M_\odot/kpc^3, & \langle \eta_\rho \rangle &\approx 0.6 \cdot 10^5(1 \pm 0.9)M_\odot/kpc^3, \\ \langle \Psi(M) \rangle &\approx 1.6\sigma_8(1 \pm 0.2). \end{aligned} \quad (32)$$

The complex internal structure of these galaxies and the significant influence of stars, discs and diffuse baryonic component restricts the number of objects for which reasonable DM characteristics can be derived. For 11 galaxies results of our analysis are presented in Figs. 1 and 2.

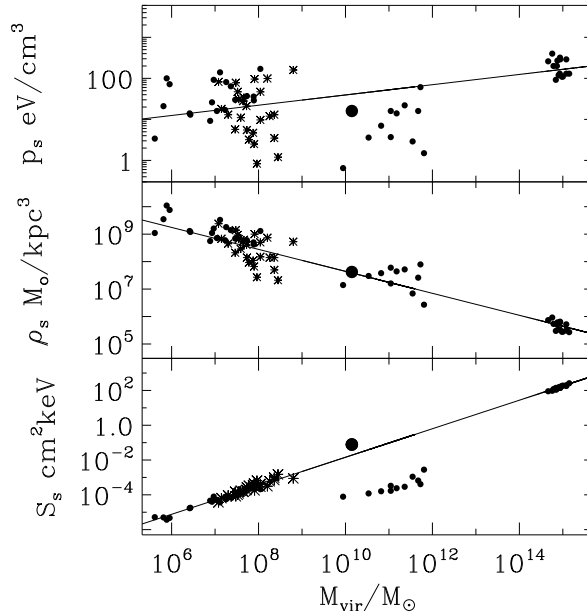


Figure 1: The functions $P_s(M_{vir})$, $\rho_s(M_{vir})$, & $S_s(M_{vir})$ are plotted for the two samples of dSph galaxies – (29) left points and (30) stars, THING and LSB galaxies (central points) and CLASH clusters of galaxies (right points). For the Dragonfly 44 values (28) are plotted by filled dark circle. Fits (33) are plotted by solid lines.

4.6 Basic characteristics of the DM cores

For two samples of dSph galaxies, Dragonfly 44 galaxy, and CLASH clusters of galaxies parameters of their DM cores (the pressure, P_s , density, ρ_s , and entropy, S_s) are plotted in Fig. 1 and are fitted by the expressions:

$$\begin{aligned}
 \langle P_s \rangle &= 140(1 \pm 0.8) \text{eV/cm}^3 M_{12}^{0.1}, \\
 \langle \rho_s \rangle &= 10^7(1 \pm 0.6) \frac{M_\odot}{\text{kpc}^3} M_{12}^{-0.45}, \\
 \langle S_s \rangle &= 0.66(1 \pm 0.4) \text{keV cm}^2 M_{12}^{0.85}, \\
 \langle 1 + z_f \rangle &= 4.1(1 \pm 0.17) M_{12}^{-0.077},
 \end{aligned} \tag{33}$$

where again $M_{12} = M_{vir}/10^{12} M_\odot$. For comparison in Fig. 1 the same functions are also plotted for THING and LSB galaxies. Large deviations of these parameters from the fits are caused by uncertainties in estimates of the influence of baryonic component and other parameters of the DM cores. Large scatter of the functions (33) reflects mainly the large scatter of the observational data and the natural random variations of object characteristics.

5 Shape of the power spectrum

Observations of the relic microwave background radiation allow to determine the shape of the initial power spectrum of density perturbations at large scales starting from clusters of galaxies (Komatsu et al. 2011; Ade et al. 2016). However, information about the power spectrum at small scale and composition and properties of dark matter is still missing. In this section we consider in more details the function $\Psi(M_{vir})$ introduced by (14) and link its mass variations with the shape of the power spectrum.

5.1 Theory versus observations

Both simulations and observations show that characteristics of the DM dominated halos are much more stable than characteristics of the baryonic component, and they can be used to characterize the small scale power spectrum of density perturbations. Indeed our analysis performed in sections 3 & 4 shows that we can find a one to one correspondence between the observed parameters of the DM halos and the redshift of object formation, z_f . According to the present day models of halo formation (Press,

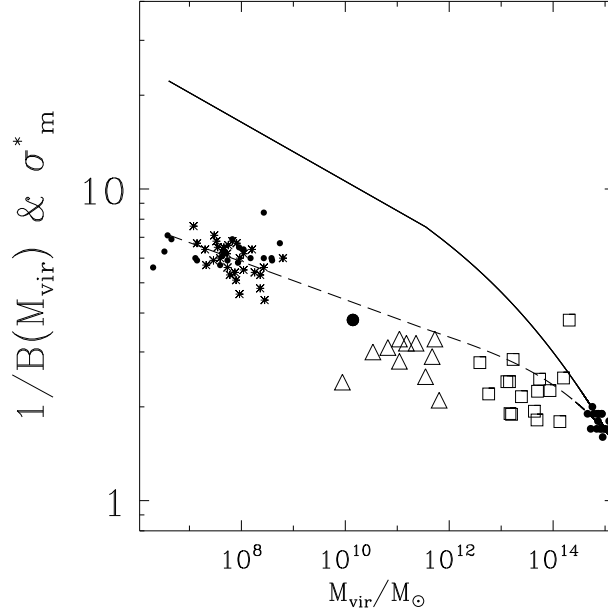


Figure 2: Dispersion of the density perturbations $\sigma_m^* = \sigma_m(M)/0.43$ (15, 34) for the standard Λ CDM power spectrum (17) and the combined spectrum (36) are plotted by solid and long dashed lines vs. M_{vir}/M_\odot . Function $B^{-1}(M_{vir})$ (2) is plotted for the two samples of dSph galaxies (left group of points and stars), for Dragonfly 44 galaxy (filled circle) and for CLASH clusters of galaxies (right group of points). For THINGS and LSB galaxies and for groups of galaxies the functions $B^{-1}(M_{vir})$ are plotted by triangles and squares.

Schechter, 1974; Peebles 1980; Bardeen et al. 1986; Bond et al. 1991; Sheth & Tormen 2002, 2004) the variations of redshift z_f with the virial mass of created objects characterize both the power spectrum of density perturbations and the real period of objects formation. As was discussed above in these models the redshift of object formation, z_f , is a weak function of virial mass. Therefore we can expect that the function $\Psi(M_{vir})$ describing this process shows also weak dependence upon the virial mass. However, estimates (27) – (32) demonstrate unexpectedly significant mass dependence of this function.

$$\langle \Psi(M) \rangle / \sigma_8 \approx 0.4, 0.74, 1.6, 1.1, 1.1, 1.1.$$

This effect suggests a possible deviation of the small scale power spectrum from that observed at larger scales by the WMAP and Planck missions and now accepted in the Λ CDM cosmological model.

This effect is illustrated in Fig. 2 where the function $B^{-1}(M_{vir})$ (2) is plotted for the samples of CLASH clusters, groups of galaxies, THING and LSB galaxies and for two samples of dSph galaxies. These functions are compared with the dispersion of the density perturbations $\sigma_m(M_{vir})$ (15) calculated for the standard Λ CDM power spectrum (17). To more clearly represent the trend we plot in Fig. 2 the function

$$\sigma_m^* = \sigma_m(M_{vir})/0.43, \quad (34)$$

that satisfies the condition

$$\Psi^*(M_{vir}) = \sigma_m^*(M_{vir})B(z_f(M_{vir})) \approx 1, \quad (35)$$

for the CLASH clusters of galaxies. The strong differences between observations and expectations of the standard CDM-like power spectrum are clearly seen in Fig. 2.

At the same figure the observed points $B^{-1}(M_{vir})$ are well fitted by functions $\sigma_m^* = \sigma_m/0.43$ obtained for the more complex power spectrum

$$p_m(k) = 0.1p_{cdm}(k) + 0.9p_{wdm}(k), \quad \sigma_m^2 = 0.1\sigma_{cdm}^2 + 0.9\sigma_{wdm}^2. \quad (36)$$

Here $p_{cdm}(k)$ is the standard CDM power spectrum. The function

$$\sigma_{wdm} \approx 1.3\sigma_8 / (1 + 0.05M_{12}^{0.4}), \quad (37)$$

corresponds to the power spectrum describing the contribution of the large scale perturbations only. The three functions $\sigma_m^*(M_{vir})$ plotted in Fig. 2 are identical to each other for $M_{vir} \geq 10^{15}M_\odot$.

As an example of the power spectrum with damped small scale part (37) we use the power spectrum of WDM particles (Viel et al. 2013), namely,

$$p_{wdm}(q) \approx p_{cdm}(q)[1 + (\alpha_w q)^{2.25}]^{-4.46}, \quad (38)$$

$$q = \frac{k}{\Omega_m h^2}, \quad \alpha_w = 6 \cdot 10^{-3} \left(\frac{\Omega_m h^2}{0.12} \right)^{1.4} \left(\frac{1keV}{m_w} \right)^{1.1},$$

where $m_w \sim (50 - 100)eV$ and the comoving wave number k is measured in Mpc^{-1} . This mass of m_w corresponds to the damping scales M_{dmp} and D_{dmp}

$$\sigma_{wdm}(M_{dmp}) = 0.5\sigma_{wdm}(0), \quad M_{dmp} = 1.8 \cdot 10^{15} M_\odot, \quad D_{dmp} \sim (10 - 20)h^{-1} Mpc. \quad (39)$$

Let us note however that in p_{wdm} and σ_{wdm} the mass m_w is only a formal parameter allowing to introduce the suitable damping scales M_{dmp} and D_{dmp} in the function σ_{wdm} (37) and such particles need not really exist. The function σ_{wdm} (37) is weakly sensitive to the shape of the spectrum (38), when the suppression of power occurs sufficiently rapidly. For example, the spectrum with the Gaussian damping

$$p_{wdm}(q) \approx p_{cdm}(q)[1 + \exp(q^2/q_{dmp}^2)]^{-2}, \quad (40)$$

and a suitable value q_{dmp} provides the same σ_{wdm} (37). At the same time the CDM-like shape of the small scale power spectrum is preserved in (36), what is consistent with similarity of the expressions (17) and (13) for $M_{12} \leq 1$. It is apparent that such decrease of the amplitude of small scale perturbations eliminates discrepancy between estimates of the function $\Psi(M_{vir})$.

5.2 'Too Big To Fail' approach

Essential support for our inferences comes from comparison of the circular velocities of simulated low mass galaxies and observed dSph satellites of Milky Way and Andromeda (Boylan–Kolchin et al. 2012; Garrison–Kimmel et al., 2014a,b; Tollerud et al. 2014; Hellwing et al. 2015; Brook, & Cintio 2015). It demonstrates that the circular velocities of objects in simulations performed with the standard Λ CDM power spectrum reproduce observations for more massive objects, but regularly overestimate the observed circular velocities for less massive objects.

It seems that this discrepancies can be related to efficiency of the environmental processes and complex evolutionary history in the context of the hierarchical formation of objects. This problem is discussed by Wetzel et al. (2015). But the similar effects are observed also for galaxies in the Local Group, where, in particular, there is the deficit of low mass galaxies in observations as compared with predictions of the standard simulations (Klypin et al. 2015). However, simulations with the standard WDM power spectrum do not reproduce observations.

These results show that more complex improvements of the standard theoretical models are required. But these indications of qualitative disagreements between standard simulations and observations are not yet followed by quantitative estimates of required corrections.

6 Discussions and conclusions

In this paper we propose a new approach that could solve some important problems of modern cosmology:

1. Explain the self similarity of the internal structure of virialized DM dominated objects in a wide range of masses, what is manifested as the regular dependence of the central pressure, density, entropy and the epoch of DM halos formation (21, 33) on the virial mass of objects.
2. Explain unexpectedly weak dependence of the DM pressure in halos on their virial masses.
3. Establish the real composition of dark matter and the shape of the small scale power spectrum of density perturbations.

Summing up let us note that the proposed approach allows us to consider and to compare properties of the observed DM dominated objects in an unprecedentedly wide range of masses $10^6 \leq M_{vir}/M_\odot \leq 10^{15}$. The main results plotted in Fig. 1 unexpectedly favor the regular self similar character of the internal structure of these objects, what confirms the main expectations of the NFW model and the regular character of the power spectrum without sharp peaks and deep troughs.

On the other hand as is seen from Fig. 2 our results favor the models with more complex power spectrum with significant excess of power at cluster scale and/or, alternatively, deficit of power at dwarf galactic scales. Both alternatives seem to be quite important and call for more detailed observational study of DM dominated objects. Our results supplement the traditional investigations of galaxies at high redshifts (see, e.g., Bouwens et al., 2015; Ellis et al. 2016).

Of course these results cannot be considered as a strong indication that the standard Λ CDM model should be modified, but they demonstrate again some intrinsic problems of this model. The strong links of DM characteristics of observed relaxed objects with the initial power spectrum and cosmological model is well known. Results presented in Figs. 1 and 2 demonstrate the regular correlations of properties of DM component with the virial masses of the relaxed objects. These correlations can be successfully interpreted in the framework of the standard model of halo formation based on the excursion set approach, but applied to a more complex power spectrum. However, these unexpected results should be tested with suitable set of high resolution simulations before their real status could be accepted.

Of course the observational base used in our discussion is very limited and it should be extended by more observations of objects with masses $M \leq 10^{12} M_{\odot}$, what may be crucial for determination of the shape of the initial power spectrum, the real composition of dark matter and even the models of inflation. Unfortunately more or less reliable estimates of the redshift z_f can be obtained mainly for the DM dominated objects or for objects with clearly discriminated impact of DM and baryonic components. The most promising results can be obtained for the mentioned in section 4 population of Ultra Diffuse Galaxies now represented by the galaxy Dragonfly 44 only (see Figs 1 & 2). We hope that the list of possible appropriate candidates will be extended.

Here we consider a phenomenological model of the power spectrum that is composed of fraction $g_{cdm} \sim 0.1 - 0.2$ of the standard CDM spectrum and fraction $g_{wdm} \sim 0.9 - 0.8$ of the HDM spectrum with the transfer function (38). Unexpectedly in the spectrum (36) the contribution of low mass particles with relatively large damping scale (39) dominates, what can be considered as reincarnation in a new version of the earlier rejected HDM model. Further progress can be achieved with more complex models of the power spectrum and/or more realistic transfer functions instead of (38, 40), what implies also more realistic complex composition of the DM component. However, all such problematic multi parametric proposals should be considered in the context of the general cosmological and inflationary models.

6.1 Acknowledgments

This paper was supported in part by the grant of the President of RF for support of scientific schools NSh-6595.2016.2. We thank S. Pilipenko, A. Klypin for useful comments.

References

- [1] Ade, P., Aghanim, N., Arnaud, M., et al. (2016) *A&A*, 594, 13
- [2] Bardeen J.M., Bond J.R., Kaiser N., & Szalay A. (1986) *ApJ*, 304, 15
- [3] Beasley, M., Romanowsky, A., Pota, V., et al. (2016) *ApJ*, 819, L20
- [4] Bond, R., Cole, S., Efstathiou, G., Kaiser, N. (1991) *ApJ*, 379, 440
- [5] Bouwens, R., Illingworth, G., Oesch, P. et al. (2015a) *ApJ*, 811, 140
- [6] Boylan-Kolchin, M., Bullock, J., Kaplinghat, M. (2012) *MNRAS*, 422, 1203
- [7] Brook, C., Cintio, A. (2015) *MNRAS*, 450, 3920
- [8] Bryan, G., Norman, M. (1998) *ApJ*, 495, 80
- [9] Burkert A. (1995) *ApJ*, 447, L25
- [10] Collins, M., Chapman, S., Rich, R., et al. (2014) *ApJ*, 783, 7
- [11] de Blok, W., Walter, F., Brinks, E., et al. (2008) *AJ*, 136, 2648
- [12] Demiański, M., Doroshkevich, A. (1999) *ApJ*, 512, 527
- [13] Demiański, M., Doroshkevich, A. (2004) *A&A*, 422, 423

- [14] Demiański, M., Doroshkevich, A., Pilipenko, S., Gottlöber, S. (2011) MNRAS, 414, 1813.
- [15] Demiański, M., Doroshkevich, A. (2014) MNRAS, 439, 179
- [16] Demiański, M & Doroshkevich, A. (2015) arXiv:151107989
- [17] Doroshkevich A., Zel'dovich, Ya. (1981) JETP, 80, 801
- [18] Ellis, J., Garcia, M., Nanopulos, D., Olive, K. (2016) CQGra, 33i4001
- [19] Garrison-Kimmel, S., Boylan-Kolchin, M., Bullock, J., Kirby, E. (2014a) MNRAS, 444, 222
- [20] Garrison-Kimmel, S., Horiuchi, S., Abazajian, K., et al. (2014b) MNRAS, 444, 961
- [21] Hellwing, W., Frenk, C., Cautun, M., et al. (2016) MNRAS, 457, 3492
- [22] Hinshaw G., Larson, D., Weiland, J., et al. (2013) ApJS, 208, 19
- [23] Karachentsev, I., Makarova, L., Makarov, D. et al. (2015) MNRAS, 337, L85
- [24] Kirby, E., Bullock, J., Boylan-Kolchin, M. (2014) MNRAS, 439, 101
- [25] Klypin, A. Karachentsev, I., Makarov, D., Nasonova, O. (2015) MNRAS, 454, 1798
- [26] Klypin, A. Trujillo-Gomez, S., Primack, J. (2011) ApJ, 740, 102;
- [27] Komatsu, E., et al. (2011) ApJS, 192, 18
- [28] Kravtsov, A., Borgani, S. (2012) ARA&A, 50, 353
- [29] Kuzio de Naray, R., Mcgaugh, S., de Blok, W. (2008) ApJ, 676, 920
- [30] Lacey, C., & Cole, S. (1993) MNRAS, 262, 627
- [31] Liu, C., Peng, E., Cote, P., et al. (2015) ApJ, 812, L34
- [32] Makarov, D., Karachentsev, I. (2011) MNRAS, 412, 2498
- [33] Mantz, A., Allen, S., Morris, R., et al. (2014) MNRAS, 440, 2077
- [34] Martinez-Delgado, D., Lasker, R., Sharina, M., et al. (2016) AJ, 151, 96
- [35] Merten, J., Meneghetti, M.; Postman, M., et al. (2015) ApJ, 806, 4
- [36] Navarro J.F., Frenk C.S., & White S.D.M. (1997) ApJ, 490, 493
- [37] Partridge R.B., & Peebles P.J.E. (1967a) ApJ, 147, 868
- [38] Partridge R.B., & Peebles P.J.E. (1967b) ApJ, 148, 377
- [39] Peebles P.J.E. (1967) ApJ, 147, 859
- [40] Peebles P.J.E. (1980) The Large-Scale Structure of the Univers, (Princeton: Princeton Univ. Press)
- [41] Press, W., Schechter, P. (1974) ApJ, 187, 425
- [42] Sheth, R., Tormen, G. (2002) MNRAS, 329, 61; (2004) MNRAS, 350, 1385
- [43] Tollerud, E., Beaton, R., Geha, M., et al. (2012) ApJ, 752, 45
- [44] Tollerud E., Boylan-Kolchin, M., Bullock, J. (2014) MNEAS, 440, 3511
- [45] Umetsu, k., Medezinski, E., Nonino, M., et al. (2014) ApJ, 795, 163
- [46] van Dokkum, P., Abraham, R., Brodie, J., et al. (2016) ApJ. 828, L6
- [47] Viel, M., Becker, G., Bolton, J., Haehnelt, M. (2013) PhRvD, 88d3502
- [48] Walker, M., Mateo, M., Olszewski, E., et al. (2009) ApJ., 704, 1274
- [49] Walker, M., Penarrubia, J. (2011) ApJ, 742, 20
- [50] Weisz, D., Skillman, E., Hidalgo, S., et al. (2014) ApJ, 789) 24
- [51] Wetzel, A., Deason, A., Garrison - Kimmel, S. (2015) ApJ, 807, 49
- [52] Zel'dovich Ya.B., Novikov I.D. (1983) Structure and evolution of the Universe, University of Chicago Press.